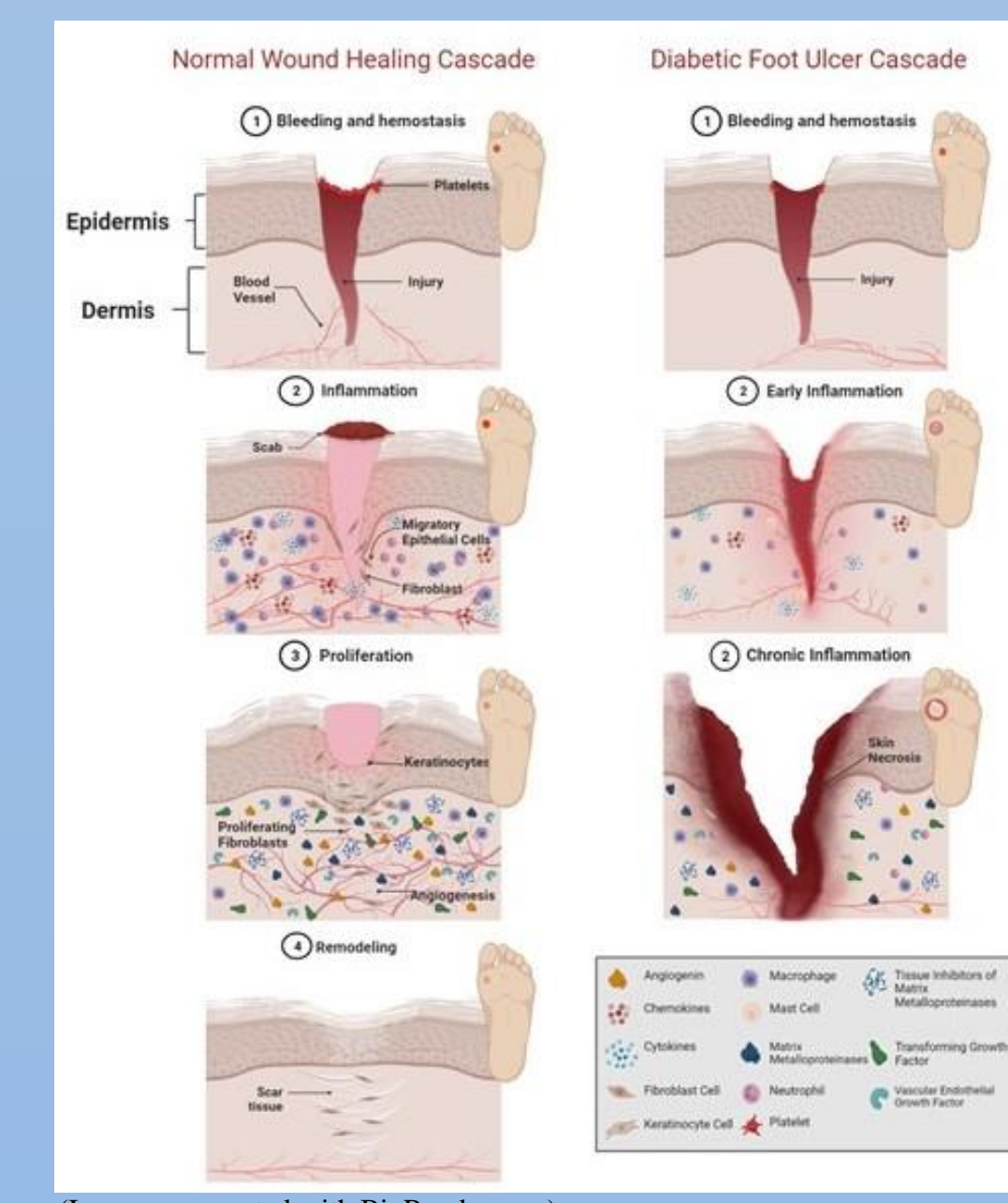




## Introduction

Biologics in regenerative medicine is a rapidly growing field that provides some of the most promising avenues to produce significant improvements in patient outcomes and comfort in the treatment of mechanical stress and injury, wear and tear, burns, surgical resections, trauma, and chronic wounds. Amnio Technology is a clinical phase regenerative medicine company focusing on technologies that improve patient outcomes. In this presentation, we focus on an innovative product and the technologies developed through evidence-based research that can be provided to patients suffering from chronic wounds. For instance, our product is an injectable derived from micronized human amniotic membrane and components from amniotic fluid. This novel birth tissue injectable is rich in cytokines and growth factors described in peer-reviewed literature as anti-inflammatory, anti-fibrotic, angiogenic and proliferative that facilitate, support, and accelerate soft tissue repair. Ultimately, we demonstrate on a molecular level how our product can reactivate and support the body's innate potential to heal and improve quality of life.



**Figure 1.** Comparison of the wound healing cascade in a normal wound versus a diabetic foot ulcer. As shown on the left, a normal wound healing cascade completes all four stages of healing: hemostasis, inflammation, proliferation, and remodeling. Higher quantities of extracellular matrix proteins, chemokines, growth factors, immune cells, and cytokines required for wound healing can be seen in a normal wound. As the wound healing continues, an overlap of the inflammatory and proliferation stage promotes angiogenesis and the proliferation of endothelial cells. The large vascular network enhanced by angiogenesis aids in wound closure and scar tissue formation. On the contrary, a diabetic foot ulcer lacks the proper vasculature to deliver the necessary proteins needed to close a wound and remain in a chronic inflammatory state despite available interventions. As a result, the ulcer continues to worsen leading to tissue necrosis.

## Methods

The focus of this study is to demonstrate the correlation between our product and the biological mechanisms that stimulate the regenerative functions of wound healing. The protein composition and elution of our product was characterized by colorimetric Bicinchoninic Acid Array (BCA) and Quantibody Human Cytokine array to quantify the concentration of multiple human inflammatory factors, growth factors, chemokines, receptors, and cytokines. Furthermore, potential proteins involved in wound healing were identified by liquid chromatography with tandem mass spectrometry (LC-MS/MS) and the raw spectral files were subjected to SEQUEST software analysis to match peptides to known protein sequence databases. A series of quantitative and qualitative *in vitro* bioassays on human dermal fibroblast (hDFa) cells were performed to determine the capabilities of our product in cellular proliferation, viability and migration. In addition, the angiogenic effects of PalinGen<sup>®</sup> Flow on tube formation using human umbilical vein endothelial cells (hUVECs) was evaluated by conducting an *in vitro* angiogenesis assay. ImageJ with Angiogenesis Analyzer plugin was used to conduct quantitative analysis on the master junctions, master segments, and meshes (tube formations) found in PalinGen<sup>®</sup> Flow. Lastly, the accurate dose delivery and rheometric properties of our product for its use as a birth tissue injectable through a 22-gauge needle was evaluated by measuring the relative potency, protein concentration, and viscosity before and after injection.

## Results

The results of the Quantibody Human Cytokine array and LC-MS/MS analysis identified multiple proteins known to influence the process of wound healing. A description of the putative function in chronic wound healing for these proteins is listed on Table 1 and 2. The *in vitro* bioassays performed on our novel birth tissue injectable PalinGen<sup>®</sup> Flow, highlight the growth in hDFa cellular proliferation, viability and migration. In addition, quantitative analysis of the master junctions, master segments, and meshes (tube formations) showed PalinGen<sup>®</sup> Flow to promote angiogenesis in hUVEC cells. Finally, it was demonstrated that the administration of PalinGen<sup>®</sup> Flow through a 22-gauge needle does not alter the composition of the final product.

**Table 1.** Quantibody protein characterization of PalinGen<sup>®</sup> Flow.

Classification	Protein	Putative Function in Chronic Wound Healing
Matrix Metalloproteinase Inhibitors	TIMP-1	Plays role in ECM composition and wound healing [1].
	TIMP-2	Enhances wound healing by stimulating cellular propagation and migration [2].
	IGFBP-1	Regulates IGF-I in DNA synthesis and wound healing, stimulating hDFa cell migration [3].
	IGFBP-2	Regulates IGF-II in DNA synthesis and wound healing. Stimulates hDFa cell migration [3].
	IGFBP-3	Ubiquitous in plasma, it binds to fibronectin, plasminogen and IGF-I [4].
	IGFBP-4	Stabilizes IGF-I to stimulate cell differentiation and proliferation [5].
Insulin-like Growth Factor Binding Proteins	IGFBP-4	Regulates cell proliferation, apoptosis, angiogenesis, cell migration, and fibrosis progression [6].
	IGFBP-6	
	OPN	Responsible for recruiting inflammatory cells to site of injury. Promotes cell adhesion and migration [7].
Glycophosphoprotein	ANG	Regulates angiogenesis. Promotes endothelial cell growth, migration, and differentiation [8].
Ribonuclease	LCN-2	Possesses antibacterial and anti-inflammatory properties. Regulates ECM degradation [9].
Glycoprotein	GDF-15	Promotes adaptive angiogenesis [10].
Transforming growth factor-β superfamily protein	ICAM-1	Promotes/regulates cell migration and proliferation. Involved in efferocytosis of immune and epithelial cells [11].

**Table 2.** Proteins identified in PalinGen<sup>®</sup> Flow Amniotic Fluid Component by LC-MS/MS and SEQUEST analysis.

Classification	Protein	Matching Peptides (SEQUEST)	Putative Function in Chronic Wound Healing
Extracellular Matrix Proteins	Fibronectin	21	ECM adhesive glycoprotein involved in re-epithelialization [12].
	Vitronectin	3	ECM adhesive glycoprotein aids in promotion of cell adhesion and spreading [13].
Regulatory Proteins	Calmodulin	3	Mitogen [14].
	IL-1 Receptor Antagonist Protein	3	Anti-inflammatory [15].
	Plasminogen	9	Precursor to plasmin, degradation of fibrin clots [16].
Functional Enzymes	Angiotensinogen	3	Precursor to angiotensin, keratinocyte and fibroblast migration [17].

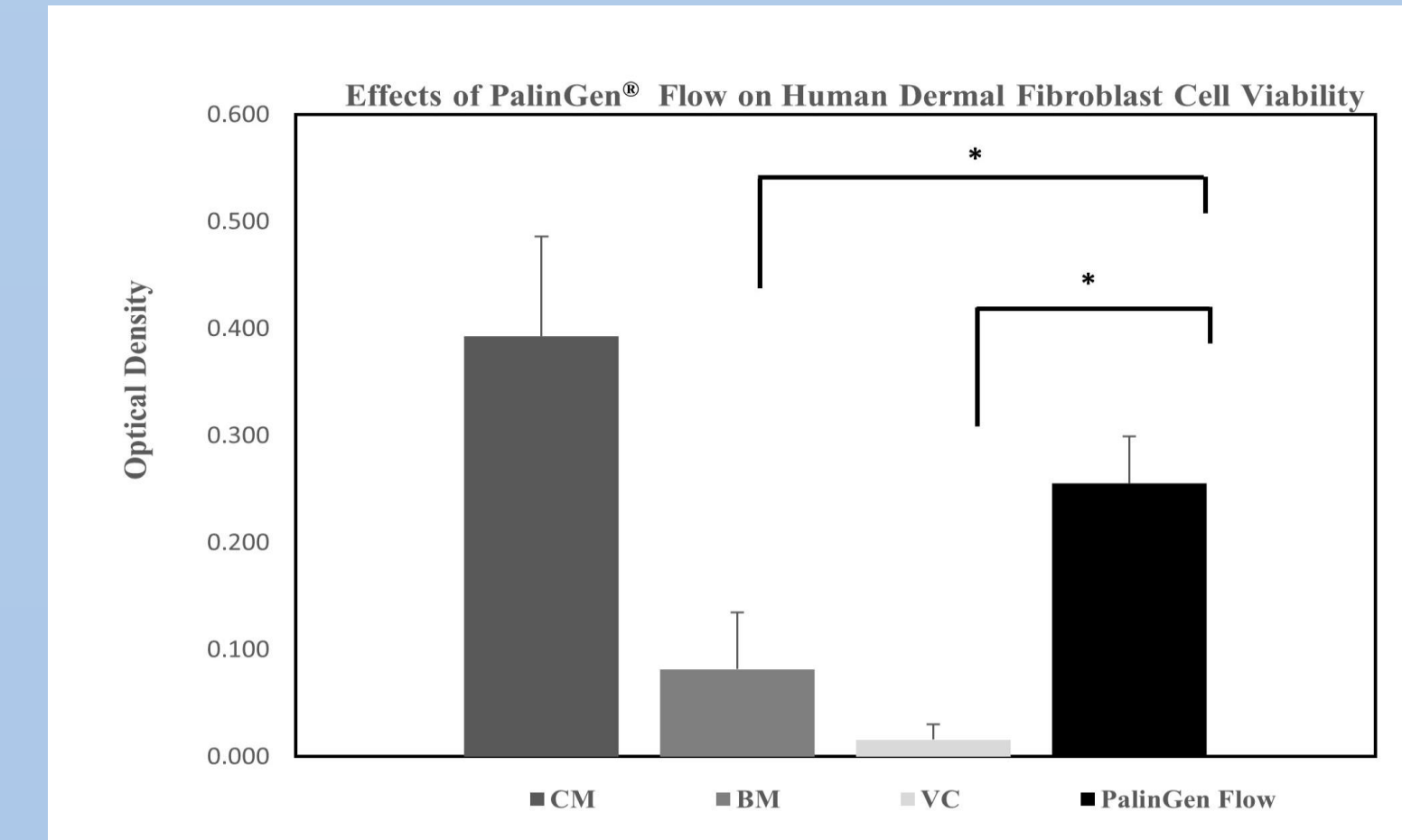


**Figure 2.** Effect of PalinGen<sup>®</sup> Flow on hDFa cell viability. The average optical densities for the hDFa cell treatments were 0.393 with a STD  $\pm$  0.093 when treated with the positive control (CM), 0.082 with a STD  $\pm$  0.053 when treated with the negative control (BM), 0.016 with a STD  $\pm$  0.014 when treated with the vehicle control (VC) and 0.255 with a STD  $\pm$  0.044 when treated with PalinGen<sup>®</sup> Flow. The average hDFa cell viability between PalinGen<sup>®</sup> Flow and either the negative or vehicle control were found to be statistically significant. A one-way ANOVA was conducted, the \*p-value <0.0001.

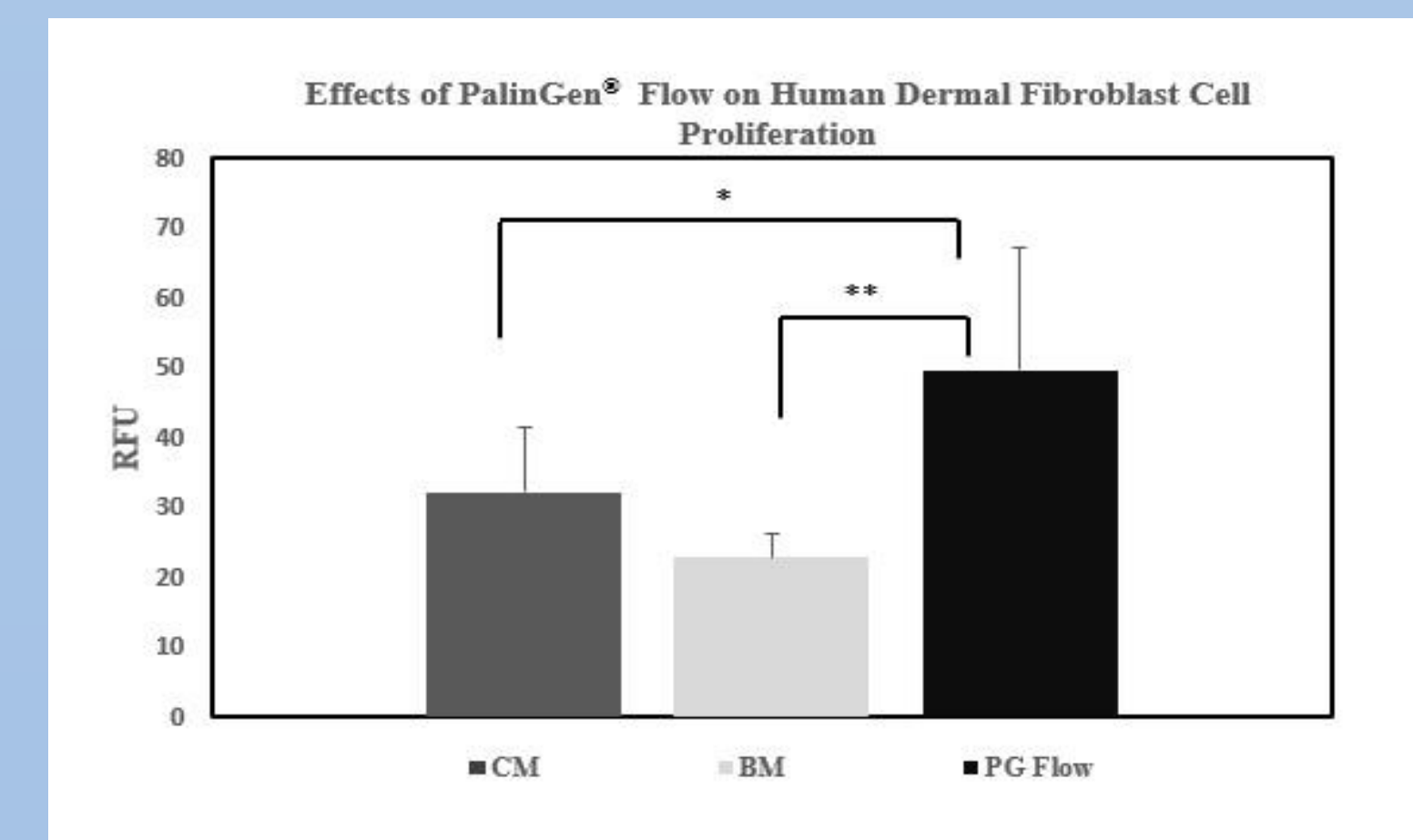


**Figure 3.** Effect of PalinGen<sup>®</sup> Flow on the proliferation of hDFa cells. The positive control (CM), negative control (BM), and PalinGen<sup>®</sup> Flow (PG Flow) samples were tested in triplicate and averaged to obtain N=3. The complete media positive control measured an average of 32 RFU with a STD  $\pm$  9, the basal media negative control measured an average of 23 RFU with a STD  $\pm$  3 with a STD  $\pm$  9.3. E) Average number of master segments formed in negative control BM, 27 with a STD  $\pm$  17.2, positive control CM, 44 with a STD  $\pm$  4.4, and PG elution, 46 with a STD  $\pm$  9.3. F) Average number of meshes (tube formation) in negative control BM, 5 with a STD  $\pm$  5.3, positive control CM, 24 with a STD  $\pm$  2.9, and PG elution, 27 with a STD  $\pm$  11.7. A one-way ANOVA was conducted, the \* p-value <0.001 \*\* p-value <0.0001.

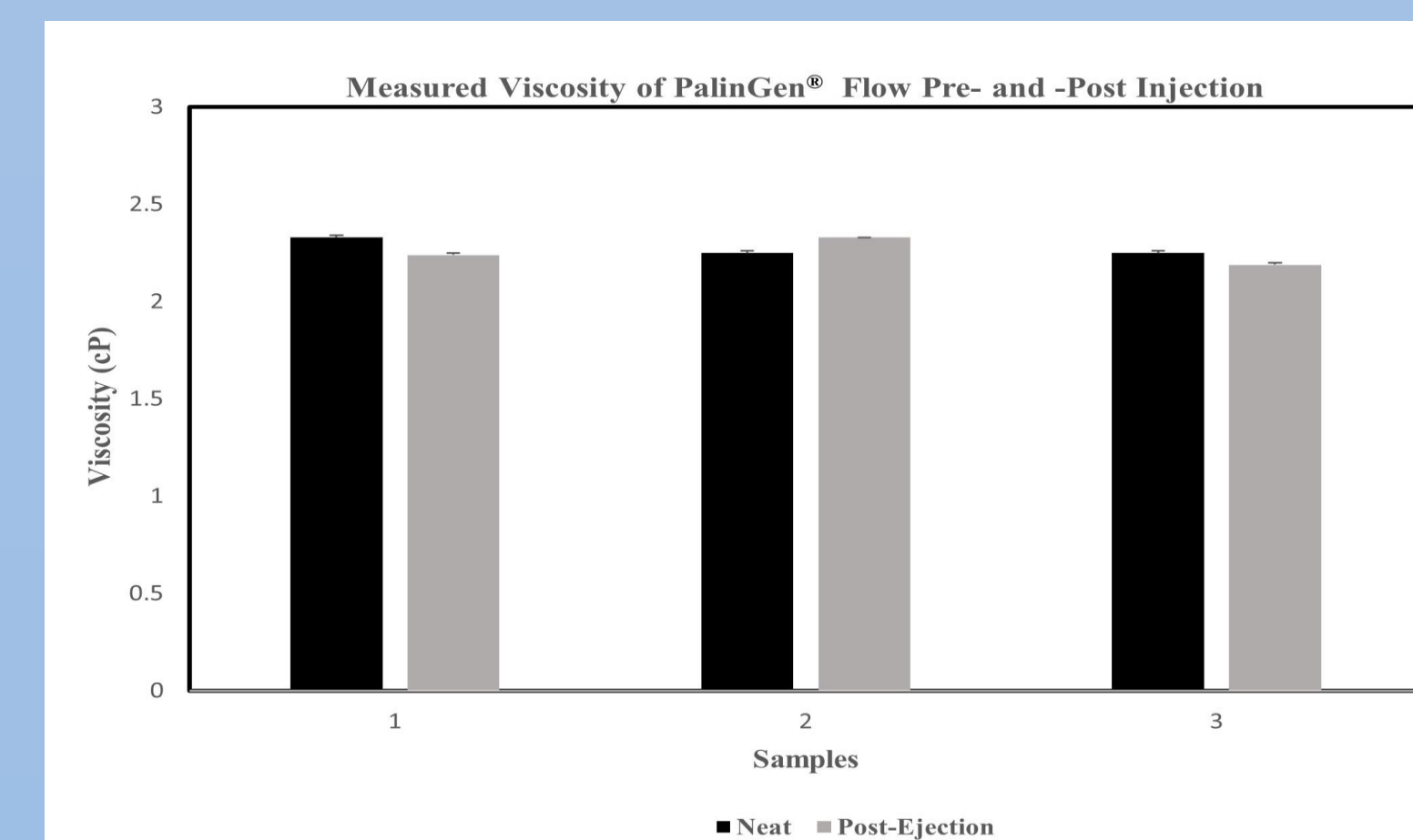


**Figure 5.** Measured viscosity, in centipoise (Cp), of PalinGen<sup>®</sup> Flow neat solutions and post-injection through a 22-gauge needle. The viscosity of three PGF samples labeled as neat solutions and after the stress of passing through a 22G needle was evaluated. A viscosity of 2.25 Cp for the neat and a 2.33 Cp for the 22G was measured for the first sample. The second sample measured 2.33 Cp neat and 2.24 Cp for the 22G and the third sample had a viscosity of 2.25 Cp for the neat and a 2.19 Cp for the 22G. Variation in viscosity of the product was negligible, < 0.15 Cp, after passing through a 22-gauge cannula.

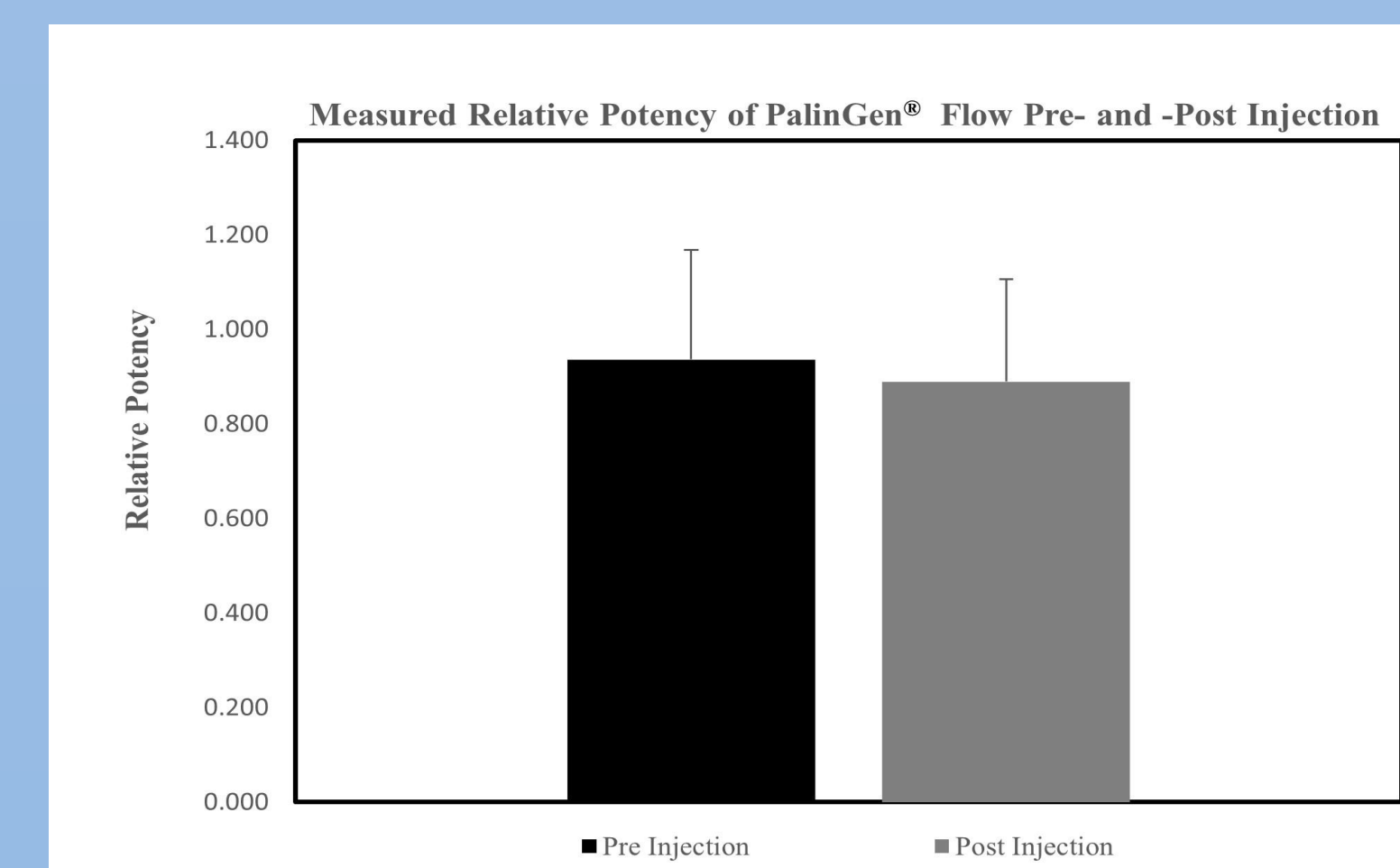


**Figure 7.** Comparison of the relative potency pre- and post- injection of PalinGen<sup>®</sup> Flow through a 22-gauge needle. Each bar represents the average of three PalinGen<sup>®</sup> Flow samples tested. The average relative potency pre-injection was 0.937 with a STD  $\pm$  0.232 and an average of 0.89 with a STD  $\pm$  0.217 post-ejection. The relative potencies of each lot measured with and without passing through the cannula were comparable and within the current product specifications.

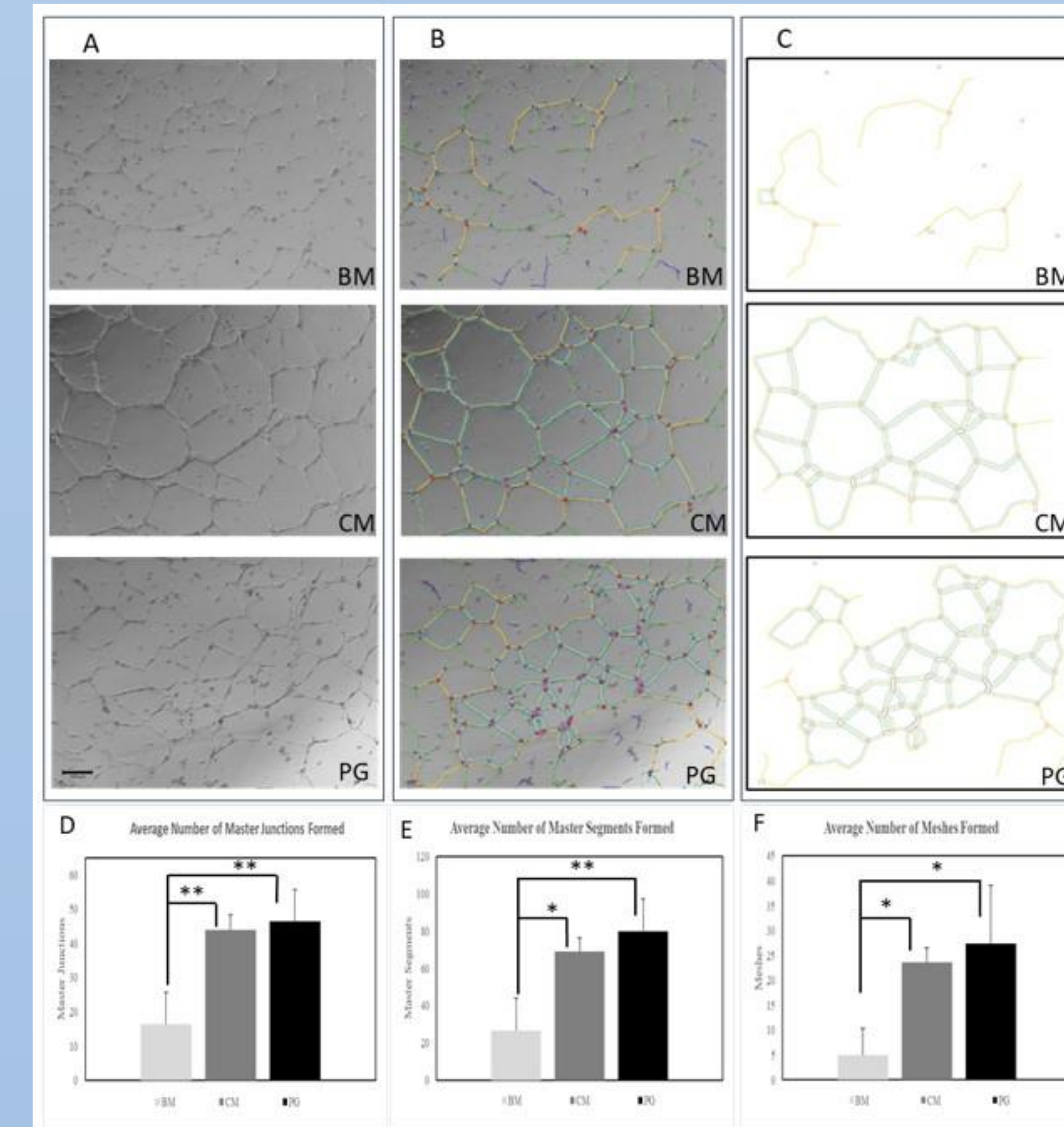


**Figure 4.** Effect of PalinGen<sup>®</sup> Flow on hUVEC tube formation. A) Phase Contrast images of negative control BM, positive control CM, and PG elution. B) Angiogenesis Analyzer images of negative control BM, positive control CM, and PG elution. C) Map images including master junctions, master segments, and meshes counted in quantitative analysis of negative control CM, positive control CM, and PG elution. D) Average number of master junctions formed in negative control BM, 16 with a STD  $\pm$  9.2, positive control CM, 44 with a STD  $\pm$  4.4, and PG elution, 46 with a STD  $\pm$  9.3. E) Average number of master segments formed in negative control BM, 27 with a STD  $\pm$  17.2, positive control CM, 44 with a STD  $\pm$  7.2, and PG elution, 80 with a STD  $\pm$  17.3. F) Average number of meshes (tube formation) in negative control BM, 5 with a STD  $\pm$  5.3, positive control CM, 24 with a STD  $\pm$  2.9, and PG elution, 27 with a STD  $\pm$  11.7. A one-way ANOVA was conducted, the \*p-value <0.05, \*\*p-value <0.01. (Scale bar = 200 μm).

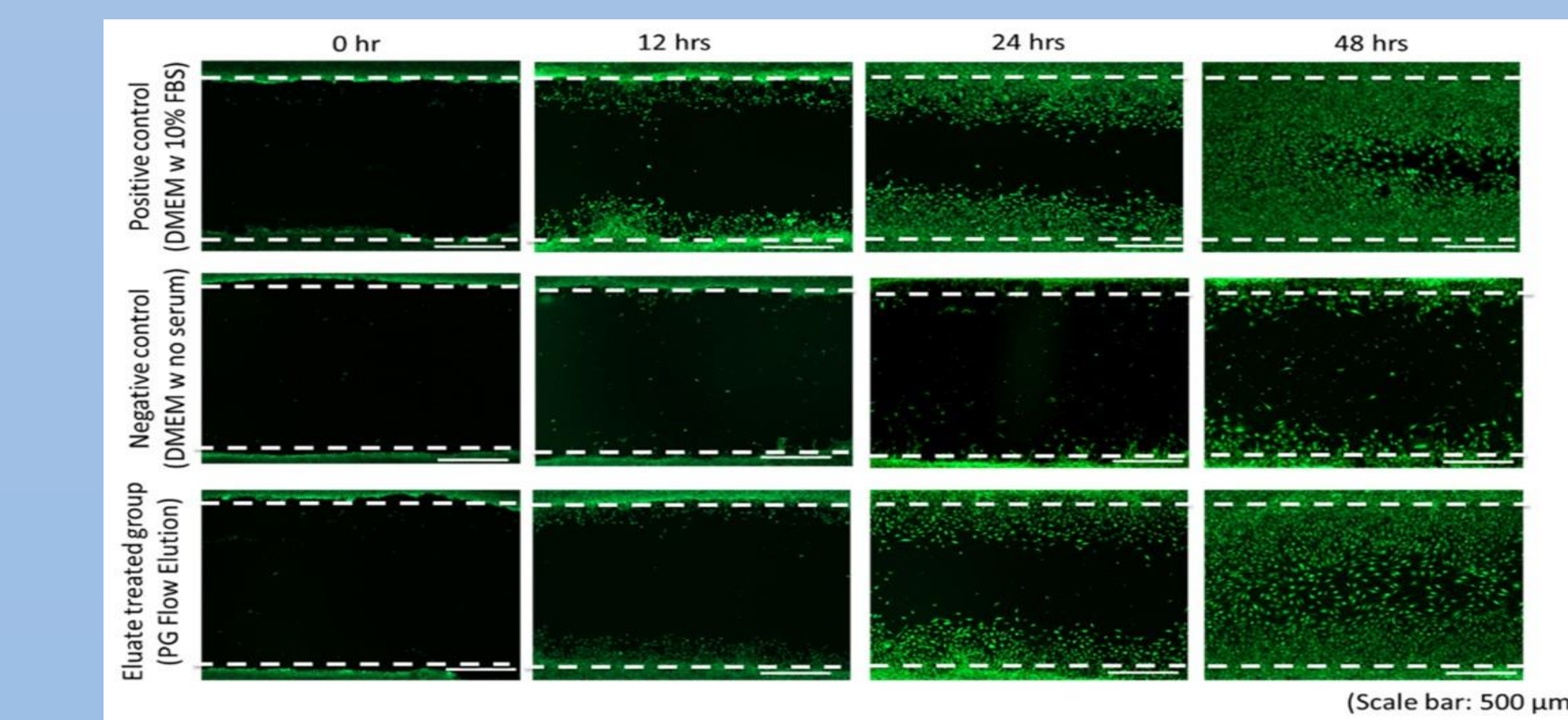


**Figure 6.** Effect of PalinGen<sup>®</sup> Flow eluates on the migration of hDFa cells. Qualitative representative images of the migration wound-healing assay at various time points (0-, 12-, 24-, and 48-hours post-treatment) were obtained. The top row shows the positive control group treated with conditioned DMEM medium, the middle row shows the negative control group treated with serum-free DMEM, and the bottom row shows the group treated with PalinGen<sup>®</sup> Flow eluates.

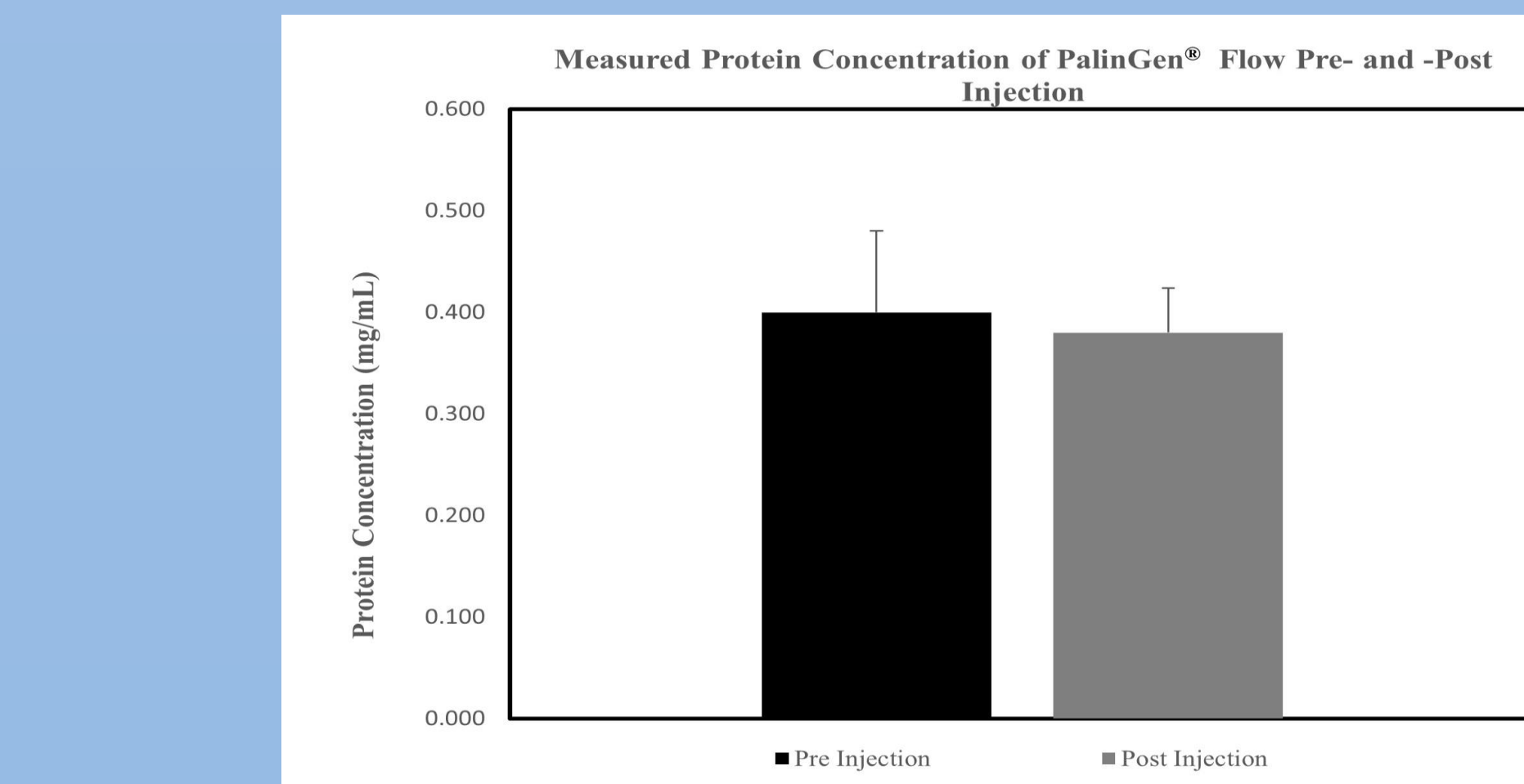


**Figure 8.** Comparison of the protein concentration pre- and post- injection of PalinGen<sup>®</sup> Flow through a 22-gauge needle. The protein concentration of PalinGen<sup>®</sup> Flow was quantified prior to and after injection through a 22-gauge needle. Each bar represents the average of triplicate samples of PalinGen<sup>®</sup> Flow tested. The average protein concentration of PalinGen<sup>®</sup> Flow pre-injection was 0.4 mg/mL with a STD  $\pm$  0.08, and post-injection, 0.38 mg/mL with a STD  $\pm$  0.04. The average protein concentrations of PalinGen<sup>®</sup> Flow were not found to be statistically significant by t-test, p=0.70.

## Clinical Trial

Presently, PalinGen<sup>®</sup> Flow is in a phase II clinical trial, NCT04667416 for the treatment for diabetic foot ulcers. Patients were treated with PalinGen<sup>®</sup> Flow in combination with standard of care every other week for 12 weeks. The DFUs shown below successfully reached full closure before the end of the 12-week study.



**Figure 9.** DFU located on sole of left foot. Patient presented with a DFU measuring an area of 0.9 cm<sup>2</sup> (Left). After two treatments of PalinGen<sup>®</sup> Flow full closure of DFU was achieved (Right).



**Figure 10.** DFU located on sole of left foot. Patient presented with a DFU measuring an area of 5.1 cm<sup>2</sup> (Left). After five treatments of PalinGen<sup>®</sup> Flow full closure of DFU was achieved (Right).



**Figure 11.** DFU located on sole of right foot. Patient presented with a DFU measuring an area of 0.9 cm<sup>2</sup> (Left). After three treatments of PalinGen<sup>®</sup> Flow full closure of DFU was achieved (Right).

## Conclusion

Our product is made of human amniotic membranes and components from amniotic fluid capable of providing a scaffold, thus acting as a protein carrier that continues to elute and deliver regenerative and functional proteins. Novel treatments like PalinGen<sup>®</sup> Flow can provide rapid wound healing, by shortening recovery time, and deliver ECM proteins, growth factors, and cytokines directly to the affected site. The *in vitro* bioassays presented support this product as an injectable composed of birth tissue for wound healing. The results conclude PalinGen<sup>®</sup> Flow is composed of many proteins shown to promote wound healing through various pathways.

## References

- Ladwig, G. P.; Rabson, M. C.; Liu, R.; Kuhn, M. A.; Mink, D. F.; Schütz, G. S. Ratio of Activated Matrix Metalloproteinase-9 to Tissue Inhibitor of Matrix Metalloproteinase-1 in Wound Fluids Are Inversely Correlated with Healing of Pressure Ulcers. *Wound Repair and Regeneration* 2002, 10 (1), 26-37. <https://doi.org/10.1086/1524-4754.2002.10981-1>.
- Tsuraki, K.; Kanaki, Y.; Aoki, T.; Iwata, K.; Saka, I. Effects of Recombinant Human Tissue Inhibitor of Metalloproteinase-2 (rhTIMP-2) on Migration of Epidermal Keratinocytes in Wound Healing. *Journal of Dermatological Science* 2003, 39 (2), 165-172. <https://doi.org/10.1016/j.jds.2003.07.002>.
- Blank, K.; Gruber, J.; Brömmer, K.; Wang, J. (2015). Effects of IGFBP-1 and IGFBP-2 and their fragments on migration and IGF-induced proliferation of human dermal fibroblasts. *Growth Hormone & IGF Research*, 25(1), 34-40.
- Gao, Y.; Shapiro, L. I. Insulin-like Growth Factor (IGF)-Binding Protein-3 (IGFBP-3) Binds to Fibronectin (FN): Demonstration of IGF-IGFBP-3/FN Ternary Complexes in Human Plasma. *The Journal of Clinical Endocrinology & Metabolism* 2001, 86 (5), 2104-2110. <https://doi.org/10.1210/endo.86.5.2104>.
- Wang, H.; Yu, R.; Wang, M.; Wang, S.; Orszag, X.; Yan, Z.; Chen, S.; Wang, W.; Wu, F.; Fan, C. Insulin-like Growth Factor Binding Protein 4 Loaded Electrospun Membrane Ameliorates Tendon Injury by Promoting Recruitment of IGF-1. *Journal of Cellular Biochemistry* 2023, 256, 162-174. <https://doi.org/10.1002/jcb.25217>.
- Lin, A.; Yamada, S.; Hata, A.; Ghallego, C.; Palumbo, G. A.; Tibello, D. IGFBP-6: At the Crossroads of Immunity, Tissue Repair and Fibrosis. *International Journal of Molecular Sciences* 2022, 23 (8), 4558. <https://doi.org/10.3390/ijms23084558>.
- Land, S. A.; Giacchetti, C. M.; Sautera, M. The Role of Osteopontin in Inflammatory Processes. *Journal of Cell Communication and Signaling* 2009, 3 (1), 311-322. <https://doi.org/10.1007/s12079-009-9060-0>.
- Choi, J.M.; Serrano, C.; Mann, T.; La Morte, D.A. Angiogenic and Copper Crossing in Wound Healing. *International Journal of Molecular Sciences* (Internet). 2021. Oct 22(21):910704. Available from: <https://doi.org/10.3390/ijms2121910704>.
- Jahedi, S. A.; Cohen, A. D.; Sousa, C.; Abdullaziz, Y. M.; Ojha, S.; Banerji, S.; Adigathe, A. A.; Licopoli, S. Structure, Function, Distribution and Role in Metabolic Disorders. *Biochimica et Biophysica Acta* 2021, 1854, 175002. <https://doi.org/10.1016/j.bba.2021.175002>.
- Roberts, L.; Ziller, M.; Combs, T.; Vargyle, C. Insights into Mechanisms of GDF15 and Receptor OGR1. *Therapeutic Targets*. *Trends in Endocrinology & Metabolism* 2020, 31 (12), 939-951. <https://doi.org/10.1016/j.tem.2020.10.005>.
- Bui, T. M.; Wisniewski, H. L.; Samraj, R. KAM-1: A Master Regulator of Cellular Responses in Inflammation, Injury Resolution, and Tumorigenesis. *Journal of Leukocyte Biology* 2020, 108 (3), 397-399. <https://doi.org/10.1002/jlb.10012020.0001>.
- Landefeld, E. A Role of Fibronectin in Normal Wound Healing. *International Journal of Cell Cloning* 2013, 12 (7), 313-316. DOI:10.1111/iccj.12109.
- Sen, A. T. M. Vitronectin Acts as a Key Regulator of Adhesion and Migration in Umbilical Cord-Derived MSCs under Different Stress Conditions. *Experimental Cell Research* 2023, 423 (2), 113467. <https://doi.org/10.1016/j.yexcr.2023.113467>.
- Wilson, Y.; Gnanaprakasam, N.; Dawson, R. A.; Smith, J.; Freudenberger, E.; Ma, N. S. Investigation of the Presence and Role of Calmodulin and Other Mitogens in Human Bone Marrow. *Journal of Bone and Joint Surgery* 1998, 15 (6), 303-314. <https://doi.org/10.1097/00006123-199807000-00004>.
- Kim, Y.; Xu, X.; Chen, C.; Samadpour, M.; Cai, T.; Zhou, Y.; Ghaheri, C.; Lu, A.; Shi, S. The Fast-Fit (FCF) Complex Regulates IL-1RA Secretion in Mesenchymal Stem Cells in Accidents Wound Healing. *Science Translational Medicine* 2018, 10 (432), ea8524. <https://doi.org/10.1126/scitranslmed.a8524>.
- Baker, S. K.; Strickland, A. A Critical Role for Plasminogen in Inflammation. *The Journal of Experimental Medicine* 2020, 217 (4), e2019185. <https://doi.org/10.1084/jem.2019185>.
- Yahara, Y.; Shirakawa, Y.; Takemura, S.; Yang, L.; Dai, X.; Toyama, M.; Tsuchi, T.; Saito, K.; Iwata, M.; Horikawa, M.; Hashimoto, K. A Novel Function of Angiogenin B in Skin Wound Healing: INDUCTION OF FIBROBLAST AND ENDOTHELIAL CELL MIGRATION BY ANGIOGENIN B IS A HEPARIN-BINDING EPIDERMAL GROWTH FACTOR (EGF) RECEPTOR-MEDIATED EGF RECEPTOR TRANSACTIVATION. *Journal of Biological Chemistry* 2006, 281 (19), 13209-13216. <https://doi.org/10.1074/jbc.M50971200>.